

## Oxygen-Bridged Iron–Copper Assemblies Pertinent to Heme–Copper Oxidases: Synthesis and Structure of an $[\text{Fe}^{\text{III}}\text{-(OH)-Cu}^{\text{II}}]$ Bridge and EXAFS Multiple-Scattering Effects of Linear Oxo and Nonlinear Hydroxo Bridges

Michael J. Scott,<sup>†</sup> Hua H. Zhang,<sup>‡</sup> Sonny C. Lee,<sup>†</sup>  
Britt Hedman,<sup>‡</sup> Keith O. Hodgson,<sup>\*,‡</sup> and R. H. Holm<sup>\*,†</sup>

Department of Chemistry, Harvard University  
Cambridge, Massachusetts 02138  
Department of Chemistry and Stanford Synchrotron  
Radiation Laboratory, Stanford University  
Stanford, California 94305

Received August 24, 1994

In the course of our development of molecular bridged assemblies relevant to the binuclear Fe/Cu (heme  $a$ -Cu<sub>B</sub>) site of heme–copper oxidases,<sup>1</sup> we have prepared the bridges  $[\text{Fe}^{\text{III}}\text{-X-Cu}^{\text{II}}]$  with  $\text{X} = \text{O}^{2-}$ ,<sup>2,3</sup> and  $\text{CN}^-$ .<sup>4</sup> The species  $[(\text{OEP})\text{Fe-O-Cu}(\text{Me}_6\text{tren})]^{+2}$  (**1**) with ground state  $S = 2$  is a plausible representation of the oxidized binuclear site in the resting state of the enzymes, while  $[(\text{py})(\text{OEP})\text{Fe-CN-Cu}(\text{Me}_6\text{tren})]^{2+}$  and related assemblies delineate the cyanide-inhibited form of the oxidized enzymes. These and other bridged species, whose bridge angles can deviate from linearity, provide especially challenging cases for multiple-scattering (MS) EXAFS analysis.<sup>5</sup> Recently, we have reported the successful use of the GNXAS analysis package to determine reliable metric information (including angles) beyond the first coordination sphere.<sup>6,7</sup> Of particular present relevance is the significant amplitude enhancement when a backscatterer and an intervening atom form a linear or near-linear relationship, such as might occur in an  $[\text{Fe-X-Cu}]$  bridge.

With oxo-bridged **1** in hand, we have sought other bridged assemblies pertinent to the binuclear enzyme site, including that with  $\text{X} = \text{OH}^-$ . Reaction of  $[\text{Cu}(\text{Me}_5\text{dien})(\text{OH}_2)](\text{ClO}_4)_2$ <sup>4c</sup> with equimolar  $\text{Li}(\text{OC}_6\text{H}_2\text{-4-Me-2,6-}t\text{-Bu}_2)$  in acetone afforded precursor compound  $[\text{Cu}(\text{Me}_5\text{dien})(\text{OH})_2](\text{ClO}_4)_2$  (**2**) as blue-green crystals (79%).<sup>8a</sup> Dimeric centrosymmetric **2** has

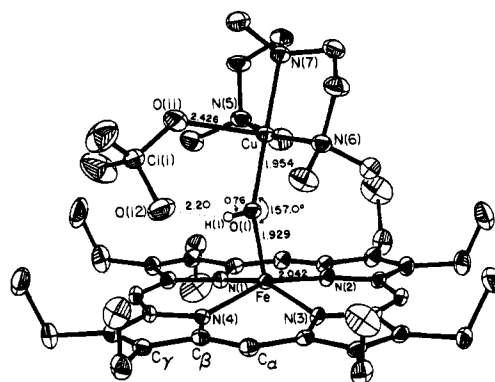


**Figure 1.** The structure of the hydroxide-bridged assembly  $[(\text{OEP})\text{Fe}(\text{OH})\text{-Cu}(\text{Me}_5\text{dien})(\text{OCIO}_3)]^+$  (**3**) showing 30% probability ellipsoids, the atom-labeling scheme, and selected bond distances (esd's 0.003–0.006 Å). Other structural parameters: Cu–N(5), 2.032(4); Cu–N(6), 2.021(4); Cu–N(7), 2.036(4); Fe–N(1–4), 2.037(4)–2.050(3); Fe–O(12), 0.44 Å; O(1)–Cu–N(7), 178.8(1)°; N(5)–Cu–N(6), 157.0(2)°; O(11)–Cu–N(5), 95.8(2)°; O(11)–Cu–N(6), 105.7(2)°; O(11)–Cu–N(7), 89.4(2)°; O(1)–Cu–N(5), 95.1(1)°; O(1)–Cu–N(6), 92.7(1)°; O(1)–Fe–N(1–4), 94.7(2)–108.2(2)°.

distorted square pyramidal (dSP) coordination with equatorial Cu–O = 1.964(4) and 1.893(5) Å, O–Cu–O = 77.2(2)°, and Cu–O–Cu = 102.8(2)°.<sup>9</sup> Reaction of 2 equiv of  $[\text{Fe}(\text{OEP})(\text{OCIO}_3)]$  with 1 equiv of  $[\text{2}](\text{ClO}_4)_2$  in dichloromethane followed by ether diffusion yielded highly crystalline dark red  $[(\text{OEP})\text{Fe}(\text{OH})\text{-Cu}(\text{Me}_5\text{dien})(\text{OCIO}_3)](\text{ClO}_4)$  (**3**) ( $[\text{3}](\text{ClO}_4)$ , 86%).<sup>8b</sup> The X-ray (XR) structure of **3** (Figure 1) demonstrates the desired hydroxo bridge. The dSP stereochemistry of **2** is retained at the Cu site, with the axial direction defined by the long Cu–O(11) distance (2.426(6) Å). The five-coordinate heme stereochemistry is clearly that of high-spin Fe(III),<sup>10</sup> with a mean Fe–N distance of 2.042(6) Å and a displacement of the Fe atom toward the bridge atom by 0.44 Å. Whereas the  $[\text{Fe}^{\text{III}}\text{-O-Cu}^{\text{II}}]$  bridge in **1** is essentially linear (175–178° in three crystalline forms<sup>2</sup>), Fe–O = 1.74 Å, and Cu–O = 1.83 Å, the  $[\text{Fe}^{\text{III}}\text{-(OH)-Cu}^{\text{II}}]$  bridge in **3** is significantly bent (157.0(2)°) and bond distances are longer. These differences are consistent with a protonated bridge; further, the bridge proton in  $[\text{3}](\text{ClO}_4)$  was located from difference Fourier maps and its positional and isotropic thermal parameters were refined. An intramolecular O(1)–H(1)···O(12) hydrogen bond appears intrinsic to the complex; both it and the bent bridge are of some generality inasmuch as they also occur in  $[\text{3}](\text{ClO}_4)_2 \cdot 1,2\text{-C}_2\text{H}_4\text{-Cl}_2$  (156.5(4)°) and  $[\text{3}](\text{SbF}_6)_2 \cdot \text{Me}_2\text{CO}$  (163.1(4)°).<sup>9</sup> Related homonuclear bridges have been established in  $\{[\text{Fe}(\text{OEP})_2\text{-(OH)}]^+\}^{11}$  and a variety of  $\text{Cu}^{\text{II}}(\mu\text{-OH})$  complexes;<sup>12</sup> bridge bond distances in **3** are in the ranges of these structures.

<sup>†</sup> Harvard University.

<sup>‡</sup> Stanford University.

(1) (a) Saratse, M. *Q. Rev. Biophys.* **1990**, *23*, 331. (b) Babcock, G. T.; Wikström, M. *Nature* **1992**, *356*, 301. (c) Chan, S. I.; Li, P. M. *Biochemistry* **1990**, *29*, 1. (d) Calhoun, M. W.; Thomas, J. W.; Gennis, R. B. *Trends Biol. Sci.* **1994**, *19*, 325.

(2) Lee, S. C.; Holm, R. H. *J. Am. Chem. Soc.* **1993**, *115*, 5833, 11789. OEP = octaethylporphyrinate(1−), Me<sub>6</sub>tren = tris(2-(N,N-dimethylamino)-ethyl)amine.

(3) A related oxo-bridged species has been prepared by others: (a) Nanthakumar, A.; Fox, S.; Murthy, N. N.; Karlin, K. D.; Ravi, N.; Huynh, B. H.; Orosz, R. D.; Day, E. P.; Hagen, K. S.; Blackburn, N. J. *J. Am. Chem. Soc.* **1993**, *115*, 8513. (b) Karlin, K. D.; Nanthakumar, A.; Fox, S.; Murthy, N. N.; Ravi, N.; Huynh, B. H.; Orosz, R. D.; Day, E. P. *J. Am. Chem. Soc.* **1994**, *116*, 4753.

(4) (a) Lee, S. C.; Scott, M. J.; Kauffmann, K.; Münck, E.; Holm, R. H. *J. Am. Chem. Soc.* **1994**, *116*, 401. (b) Scott, M. J.; Lee, S. C.; Holm, R. H. *Inorg. Chem.* **1994**, *33*, 4651. (c) Scott, M. J.; Holm, R. H. *J. Am. Chem. Soc.*, in press. Me<sub>5</sub>dien = 1,1,4,7,7-pentamethyldiethylenetriamine.

(5) The angular dependence of MS effects has been known for some time and, in favorable cases, has been used to obtain angular information; cf., e.g.: Teo, B. K. *J. Am. Chem. Soc.* **1981**, *103*, 3900. Co, M. S.; Hendrickson, W. A.; Hodgson, K. O.; Doniach, S. *J. Am. Chem. Soc.* **1983**, *105*, 1144. Binsted, N.; Cook, S. L.; Evans, J.; Greaves, N. G.; Price, R. J. *J. Am. Chem. Soc.* **1987**, *109*, 3669. To our knowledge, the GNXAS package offers the first general approach to the treatment of three-body MS signals with correlated distances and Debye–Waller factors.<sup>6</sup>

(6) Nordlander, E.; Lee, S. C.; Cen, W.; Wu, Z. Y.; Natoli, C. R.; Di Cicco, A.; Filippini, A.; Hedman, B.; Hodgson, K. O.; Holm, R. H. *J. Am. Chem. Soc.* **1993**, *115*, 5549.

(7) (a) Westre, T. E.; Di Cicco, A.; Filippini, A.; Natoli, C. R.; Hedman, B.; Solomon, E. I.; Hodgson, K. O. *J. Am. Chem. Soc.* **1994**, *116*, 6757. (b) Liu, H. I.; Filippini, A.; Gavini, N.; Burgess, B. K.; Hedman, B.; Di Cicco, A.; Natoli, C. R.; Hodgson, K. O. *J. Am. Chem. Soc.* **1994**, *116*, 2418.

(8) (a) Calcd for C<sub>18</sub>H<sub>48</sub>Cl<sub>2</sub>Cu<sub>2</sub>N<sub>6</sub>O<sub>10</sub>: C, 30.60; H, 6.85; Cu, 17.99; N, 11.89. Found: C, 30.56; H, 6.95; Cu, 17.88; N, 11.84. (b) Calcd for C<sub>45</sub>H<sub>68</sub>Cl<sub>2</sub>CuFeN<sub>7</sub>O<sub>9</sub>: C, 51.90; H, 6.58; Cu, 6.10; Fe, 5.36; N, 9.42. Found: C, 51.79; H, 6.63; Cu, 6.18; Fe, 5.47; N, 9.48.

(9) X-ray structure analyses: Data were obtained with Mo K $\alpha$  radiation and structures were solved and refined by standard methods.  $[\text{2}](\text{ClO}_4)_2$  (298 K): orthorhombic (*Pbca*),  $a = 12.827(9)$  Å,  $b = 11.876(6)$  Å,  $c = 19.850(13)$  Å, 1977 observed data ( $F_o^2 > 2\sigma(F_o)^2$ ,  $3^\circ \leq 2\theta \leq 45^\circ$ ),  $R(R_w) = 3.71(4.16)\%$ .  $[\text{3}](\text{ClO}_4)$  (298 K): triclinic (*P1*),  $a = 12.08(1)$  Å,  $b = 14.20(1)$  Å,  $c = 16.30(1)$  Å,  $\alpha = 106.17(2)^\circ$ ,  $\beta = 97.58(2)^\circ$ ,  $\gamma = 109.21(2)^\circ$ , 4234 observed data ( $F_o^2 > 3\sigma(F_o)^2$ ,  $3^\circ \leq 2\theta \leq 45^\circ$ ),  $R(R_w) = 3.30(3.52)\%$ .  $[\text{3}](\text{ClO}_4)_2 \cdot \text{C}_2\text{H}_4\text{-Cl}_2$  (223 K): triclinic (*P1*),  $a = 12.986(7)$  Å,  $b = 13.297(5)$  Å,  $c = 17.471(6)$  Å,  $\alpha = 104.82(3)^\circ$ ,  $\beta = 91.97(4)^\circ$ ,  $\gamma = 112.94(3)^\circ$ , 3217 observed data ( $F_o^2 > 2\sigma(F_o)^2$ ,  $3^\circ \leq 2\theta \leq 42.5^\circ$ ),  $R(R_w) = 6.25(15.19)\%$ .  $[\text{3}](\text{SbF}_6)_2 \cdot \text{Me}_2\text{CO}$  (223 K): triclinic (*P1*),  $a = 13.913(4)$  Å,  $b = 13.996(3)$  Å,  $c = 17.279(4)$  Å,  $\alpha = 87.84(2)^\circ$ ,  $\beta = 71.09(2)^\circ$ ,  $\gamma = 62.47(2)^\circ$ , 3648 observed data ( $F_o^2 > 3\sigma(F_o)^2$ ,  $3^\circ \leq 2\theta \leq 48^\circ$ ),  $R(R_w) = 5.04(13.19)\%$ . In the latter two compounds, the orientation of the perchlorate atom O(12) is essentially identical to that of  $[\text{3}](\text{ClO}_4)$ ; the bridge atom H(1) was not located in these cases.

(10) Scheidt, W. R.; Reed, C. A. *Chem. Rev.* **1981**, *81*, 543. The porphyrin ring is nearly planar; deviations from the least squares plane are +0.069 Å to −0.087 Å.

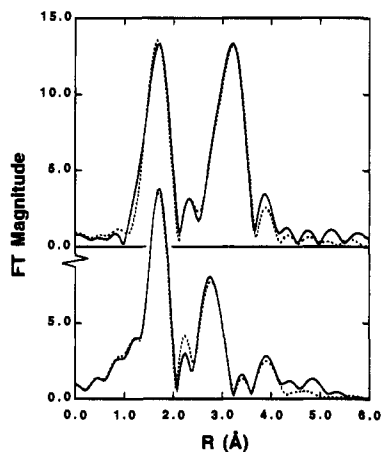


**Figure 2.** Comparison of Fourier transforms of the experimental data (—) with those of the theoretical signal (···) for **1** (upper) and **3** (lower). The Fourier transforms were performed over the  $k$ -range 4.4–14.8 Å<sup>-1</sup> and are not phase-shift corrected. The very strong MS effect of the near-linear Fe–O–Cu bridge is clearly seen in the unusually high outer-shell peak near 3.1 Å for **1**, whereas the corresponding Fe–O(H)–Cu peak at ~3.4 Å for **3** reflects the minor MS contribution due to the 157° angle.

We have used the GNXAS MS protocol<sup>6,7a</sup> to analyze EXAFS data of [**1**](ClO<sub>4</sub>) and [**3**](ClO<sub>4</sub>) at the Fe K-edge.<sup>13</sup> The EXAFS Fourier transforms (FTs) of the data and of the fit to the data are presented in Figure 2. The fits of both complexes include the two-body contributions Fe–O, Fe–N, and Fe–C<sub>α</sub> and the three-body MS components Fe–N–C<sub>β</sub>, Fe–O–Cu, and Fe–N–C<sub>γ</sub>.<sup>13</sup> The fits of **1** in addition include the Fe–C(methyl) contributions of the Me<sub>6</sub>tren ligand.<sup>2</sup> In each case, the refined EXAFS signal matches quite closely with the experimental data. The low-frequency EXAFS is well accounted for by the single scattering components Fe–O and Fe–N, which afford the first FT peak at ~1.7 Å (**1**) and at ~1.8 Å (**3**). The refined first-, second-, and third-shell distances deviate from XR values by <0.01, 0.03, and 0.04 Å, respectively. The three-body MS contribution Fe–N–C<sub>β</sub> is also relatively large because this pathway occurs eight times in the porphyrin ring; the pathway angle deviates by 3° from the X-ray data.

A dramatic difference is seen in the outer-shell region of the EXAFS FTs (Figure 2). In **1**, the enhancement of the Cu backscattering amplitude makes it even larger than the Fe–N–C<sub>β</sub> signal. Thus, the FT feature at ~3.1 Å includes a major Fe–O–Cu MS contribution which, together with the single scattering signal Fe–C<sub>α</sub>, produces an FT peak of nearly the same magnitude as the first-shell peak. This peak can be satisfactorily fitted *only* when this MS contribution is included. From GNXAS, the agreement in bridge parameters between the XR/calculated values is excellent: *e.g.*, Fe–Cu = 3.570/3.57 Å and Fe–O–Cu = 175.3°/172°. In contrast, **3** exhibits a much weaker Fe–O–Cu signal which contributes less significantly

(11) Scheidt, W. R.; Cheng, B.; Safo, M. K.; Cukiernik, F.; Marchon, J.-C.; Debrunner, P. G. *J. Am. Chem. Soc.* **1992**, *114*, 4420. Fe–O = 1.924(3), 1.952(3) Å; Fe–O–Fe = 146.2(2)°.

(12) (a) Studer, S.; Riesen, A.; Kaden, T. A. *Helv. Chim. Acta* **1989**, *72*, 307. (b) Castro, I.; Faus, J.; Julve, M.; Lloret, F.; Verdager, M.; Kahn, O.; Jeannin, S.; Jeannin, Y.; Vaisserman, J. J. *Chem. Soc., Dalton Trans.* **1990** and references therein. Cu–O = 1.85–1.93 Å; Cu–O–Cu = 128–146°.

(13) EXAFS transmission data were recorded at 10 K at the Stanford Synchrotron Radiation Laboratory (SSRL): unfocused beamline 7–3, Si-(220) double-crystal monochromator, 3.0 GeV, 60–100 mA. EXAFS signals for each of the two-body and three-body configurations were calculated on the basis of crystallographic distances and angles, but with 4mm symmetry applied to the porphyrin. Individual signals with significant contributions (see text) were summed to generate the total theoretical EXAFS signal, which was then fitted to the experimental data by varying distances, angles, Debye–Waller factors, and nonstructural parameters.<sup>6,7</sup> A total of 33 (for **1**) and 31 (for **3**) parameters were varied in the refinements; further details and final results are summarized in the supplementary material.

to the total EXAFS signal. (See supplementary material for a comparison of the relative strengths of the Fe–O–Cu MS EXAFS signals.) The longer Fe–O distance shifts the Fe–O–Cu FT peak to ~3.4 Å; the major contributor to the ~4.0 Å peak is the Fe–N–C<sub>γ</sub> MS signal. Because of the relatively weak Fe–O–Cu contribution, determination of structural parameters is less accurate but still useful; XR/calculated values are Fe–Cu = 3.804/3.89 Å and Fe–O–Cu = 157.0°/161°. The inclusion of this contribution did, however, improve the fit (the goodness-of-fit value<sup>6</sup> decreased by ~25%).

The bridge structural differences in linear **1** and nonlinear **3** give rise to dramatic changes in their EXAFS spectra. GNXAS analysis is effective in quantifying the sensitivity of the MS signals to the geometry of the bridging configuration between metal centers. As shown here and for a related case,<sup>7a</sup> *this technique is relatively sensitive and accurate when the bridge approaches linearity*. At bridge angles below *ca.* 160° in cases such as **3**, angle determination becomes less reliable and ultimately (at even lower angles) unreliable, in part due to other strong MS pathways in the porphyrin framework. However, in heme-based Fe–X–Cu bridged assemblies, porphyrin MS effects do not contribute to the Cu EXAFS; more reliable values may be anticipated for nonlinear systems, at least in the absence of imidazole ligation, for which MS effects can also be significant.

Treatment of an acetone slurry of **3** with 1.3 equiv of Li(OC<sub>6</sub>H<sub>2</sub>-4-Me-2,6-*t*-Bu<sub>2</sub>) in acetone resulted in instant dissolution and diastereotopic methylene signals ( $\delta$  17.3, 21.1) convincingly close to those of **1** in acetone ( $\delta$  17.4, 20.0<sup>2</sup>) and very different from those of **3** in CD<sub>2</sub>Cl<sub>2</sub> ( $\delta$  32.5, 42.9).<sup>8b</sup> Consequently, the latter has been deprotonated<sup>14</sup> to [(OEP)Fe–O–Cu(Me<sub>5</sub>dien)(OCIO<sub>3</sub>)] (**4**), but as yet a pure sample has not been isolated. The much larger isotropic shifts of **3** vs **1** and **4** imply weaker magnetic coupling. While [**3**](ClO<sub>4</sub>) exhibits Curie–Weiss behavior at 10–100 K and retains the  $S = 2$  ( $C = 3.10$  emu K/mol) ground state of **1**, it deviates in the direction of larger paramagnetism at higher temperatures. A fit of the magnetic susceptibility ( $\chi^M$ ) data to a coupled  $S = 1/2, 5/2$  system yields  $J \approx -80$  cm<sup>-1</sup> ( $H = -2JS_1S_2$ ), more weakly coupled than **1**, which exhibits linear  $\chi^M$  vs  $1/T$  behavior up to 300 K.<sup>2</sup> Because of the ground state of **3**, a hydroxo bridge is a viable structural element in resting enzymes.<sup>15</sup> Further research on [Fe–X–Cu] bridges will involve synthesis and spectroscopy of new bridges, Cu EXAFS of oxo/hydroxo assemblies, and applications of the EXAFS protocol to binuclear enzymic sites in different states.

**Acknowledgment.** This research was supported by NSF CHE 92-08387 (to R.H.H.) and by NSF CHE 91-21576 and NIH RR-01209 (to K.O.H.). SSRL is supported by the Department of Energy, Office of Basic Energy Sciences, and in part by the National Institutes of Health, National Center for Research Resources, Biomedical Research Technology Program, and by the DOE Office of Health and Environmental Research.

**Supplementary Material Available:** X-ray structural data for [**2**](ClO<sub>4</sub>)<sub>2</sub> and the three compounds containing **3** and EXAFS data and fit results (33 pages). This material is contained in many libraries on microfiche, immediately follows this article in the microfilm version of the journal, and can be ordered from the ACS; see any current masthead page for ordering information.

JA9428366

(14) Reversible protonation of an [Fe<sup>III</sup>–O–Cu<sup>II</sup>] bridge has been reported in a system in which the [Fe<sup>III</sup>–(OH)–Cu<sup>II</sup>] component, although structurally uncharacterized, does not contain an intramolecular hydrogen bond.<sup>3a</sup>

(15) Recently, the presence of a S or Cl atom in the first coordination sphere of both Cu and Fe in a bacterial oxidase was indicated by EXAFS analysis and interpreted as constituting the bridging ligand: Powers, L.; Laureus, M.; Reddy, K. S.; Chance, B.; Wikström, M. *Biochim. Biophys. Acta* **1994**, *1183*, 504. The authors, however, deduced that the usually short Cu–S/Cl distance makes this assignment yet to be finally established, and the generality of this result is thus not definite.